Nitric Oxide Activation of Soluble Guanylyl Cyclase Reveals High and Low Affinity Sites That Mediate Allosteric Inhibition by Calcium†

Shiva Kazerounian,*,‡ Giovanni M. Pitari,‡,⊥ Inez Ruiz-Stewart,‡ Stephanie Schulz,‡ and Scott A. Waldman‡

Division of Clinical Pharmacology, Departments of Medicine and Biochemistry and Molecular Pharmacology, Thomas Jefferson University, Philadelphia, Pennsylvania 19107, and Department of Pharmacology, University of Catania Medical School, Catania, Italy

Received May 29, 2001; Revised Manuscript Received December 4, 2001

ABSTRACT: Cyclic GMP (cGMP) and Ca^{2+} regulate opposing mechanisms in (patho)physiological processes reflected in the reciprocal regulation of their intracellular concentrations. Although mechanisms by which cGMP regulates $[Ca^{2+}]_i$ have been described, those by which Ca^{2+} regulates $[cGMP]_i$ are less well understood. In the present study, Ca^{2+} inhibited purified sGC activated by sodium nitroprusside (SNP), a precursor of nitric oxide (NO), employing Mg-GTP as substrate in a concentration-dependent fashion, but was without effect on basal enzyme activity. Ca^{2+} inhibited sGC stimulated by protoporphyrin IX or YC-1 suggesting that inhibition was not NO-dependent. In contrast, Ca^{2+} was without effect on sGC activated by SNP employing Mn-GTP as substrate, demonstrating that inhibition did not reflect displacement of heme from sGC. Ligand activation of sGC unmasked negative allosteric sites of high ($K_i \sim 10^{-7}$ M) and low ($K_i \sim 10^{-5}$ M) affinity for Ca^{2+} that mediated noncompetitive and uncompetitive inhibition, respectively. Free Mg^{2+} in excess of substrate did not alter the concentration−response relationship of Ca^{2+} inhibition at high affinity sites, but produced a rightward shift in that relationship at low affinity sites. Similarly, Ca^{2+} inhibition at high affinity sites was noncompetitive, whereas inhibition at low affinity sites was competitive, with respect to free Mg^{2+}. Purified sGC specifically bound $^{45}Ca^{2+}$ in the presence of a 1000-fold excess of Mg^{2+} and in the absence of activating ligands. These data suggest that sGC is a constitutive Ca^{2+} binding protein whose allosteric function is conditionally dependent upon ligand activation.

Soluble GC, a member of the family of signal transduction enzymes that generate cGMP[1] from GTP, is a heterodimer composed of α and β subunits. Both subunits are required for activation of sGC by ligands such as NO (*1*−*3*), which bind to a heme prosthetic group, increasing $[cGMP]_i$ and transmitting signals to downstream effectors such as cGMP-dependent protein kinases, cyclic nucleotide-gated channels, and cGMP-regulated phosphodiesterases (*4*).

Cyclic GMP and Ca^{2+} regulate important (patho)physiological mechanisms in an opposing fashion in several systems. In VSMCs, cGMP and Ca^{2+} reciprocally regulate contractility: increases in free $[Ca^{2+}]_i$ are required for contraction, whereas increases in $[cGMP]_i$ are associated with relaxation (*5*, *6*). Cyclic GMP mediates relaxation, in part, by lowering $[Ca^{2+}]_i$ by (i) decreasing influx of Ca^{2+}, (ii) increasing efflux of Ca^{2+}, (iii) promoting sequestration of Ca^{2+} in the sarcoplasmic reticulum, and (iv) attenuating mobilization of Ca^{2+} (*4*). $[cGMP]_i$ is known to be reciprocally regulated by $[Ca^{2+}]_i$. Ca^{2+} inhibited rat lung sGC heterologously expressed in HEK293 cells, and elevation of $[Ca^{2+}]_i$ reduced production of $[cGMP]_i$ in response to NO in those cells (*7*). Similarly, depolarization of pituitary cells by high K^+ or L-type Ca^{2+} channel agonists increased $[Ca^{2+}]_i$ and decreased $[cGMP]_i$ accumulation in response to NO (*8*). Also, Ca^{2+} inhibited sGC and reciprocally regulated $[cGMP]_i$ in pancreatic acinar cells (*9*). These observations suggest that $[Ca^{2+}]_i$ regulates $[cGMP]_i$, possibly by directly inhibiting sGC. However, the mechanisms by which Ca^{2+} inhibits sGC and the sites with which it interacts have not been defined.

Previous studies suggest that guanylyl cyclases possess at least two divalent cation binding sites. In the catalytic domain, a divalent cation facilitates catalysis by forming a

† These studies were supported by NIH Grant HL59214 and Targeted Diagnostics and Therapeutics, Inc. S.A.W. is the Samuel M. V. Hamilton Professor of Medicine of Thomas Jefferson University.

* To whom correspondence should be addressed. Shiva Kazerounian, Division of Clinical Pharmacology, Thomas Jefferson University, 1100 Walnut Street, Room 810, Philadelphia, PA 19107, Phone: (215) 955−9080; Fax: (215) 955−7006, E-mail: Shiva.Kazerounian@jefferson.edu.

‡ Thomas Jefferson University.

⊥ University of Catania Medical School.

[1] Abbreviations: AC, adenylyl cyclase; BSA, bovine serum albumin; $CaCl_2$, calcium chloride; $[Ca^{2+}]_i$, intracellular concentration of calcium; cGMP, (3′-5′) cyclic guanosine monophosphate; $[cGMP]_i$, intracellular concentration of cGMP; CaM, calmodulin; DTT, dithiothreitol; EDTA, ethylenediamine tetraacetic acid; EGTA, ethylene glycol-bis (β-aminoethyl ether)-*N*,*N*,*N*′,*N*′-tetraacetic acid; GCAPs, guanylyl cyclase activating proteins; GCs, guanylyl cyclases; GTP, guanosine 5′ triphosphate; K_i, concentration of ligand yielding half-maximal inhibition; K_m, concentration of substrate yielding half-maximal velocity; Me-GTP, metal-GTP; $MgC1_2$, magnesium chloride; $MnCl_2$, manganese chloride; NaAc, sodium acetate; NaCl, sodium chloride; NO, nitric oxide; PPIX, protoporphyrin IX (3,7,12,17- tetramethyl-8,13-diviinyl-2,18-porphrin-dipropionic acid); SDS−PAGE, sodium dodecyl sulfate−polyacrylamide gel electrophoresis; sGC, soluble guanylyl cyclase; SNP, sodium nitroprusside; V_{max}, maximal enzyme velocity; VSMCs, vascular smooth muscle cells; YC-1, 3-[5′-(hydroxymethyl)-2′-furyl}-1-benzylindazole.

10.1021/bi0110894 CCC: $22.00
Published on Web 02/12/2002

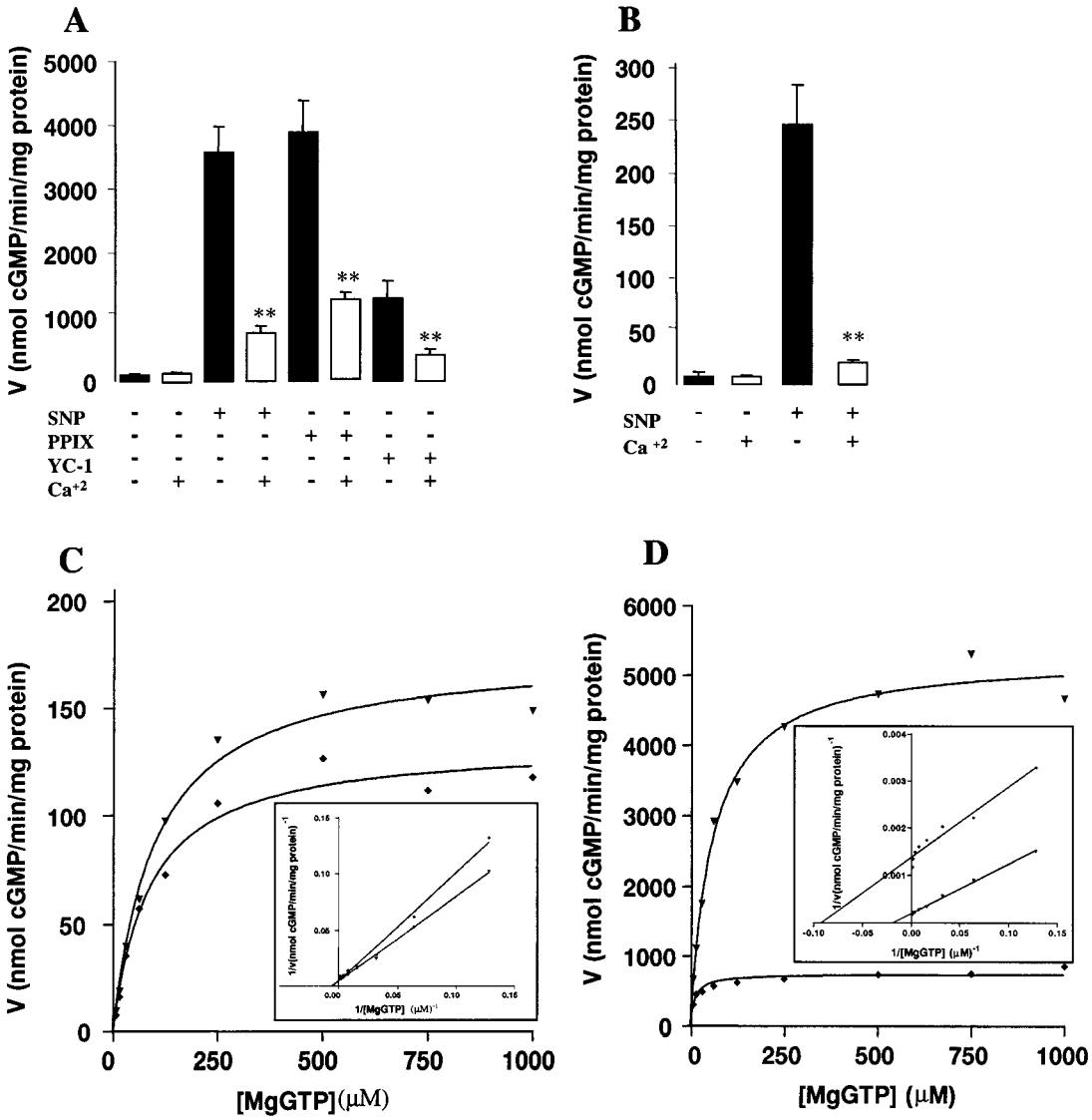

FIGURE 1: Ca^{2+} inhibition of purified sGC employing Mg-GTP as the substrate. The activity of purified sGC (5 ng) was quantified as described in Methods in incubations (37 °C, 5 min) containing (A) 100 μM Mg-GTP, 3 mM excess free Mg^{2+} and, where indicated, 50 μM SNP, 100 μM PPIX, 200 μM YC-1, or 250 μM Ca^{2+}; (B) 100 μM Mg-GTP in the absence of excess Mg^{2+} and, where indicated, 50 μM SNP or 250 μM Ca^{2+}; (C) increasing concentrations of Mg-GTP (10−1000 μM), 3 mM excess Mg^{2+} and 0 μM (▼) or 250 μM (◆) Ca^{2+}; (D) increasing concentrations of Mg-GTP (10−1000 μM), 3 mM excess Mg^{2+}, 50 μM SNP and 0 μM (▼) or 250 μM (◆) Ca^{2+}. Results are representative of ≥3 experiments performed in duplicate. **, $p < 0.01$ as compared to incubations without Ca^{2+}. Insets: linear analysis of double-reciprocal plots used to estimate V_{max} and K_m values presented in Table 1.

bridge between the enzyme and the substrate (*10*). The divalent cation binds to this site in the form of a complex with the nucleotide substrate (Me-GTP). In addition, divalent cations bind as free metal to other uncharacterized sites on the enzyme and regulate activity in a positive allosteric fashion (*11*). Indeed, divalent cations in excess of substrate (Me-GTP) are required for maximum activation of guanylyl cyclases by ligands, presumably reflecting a requirement for binding to positive allosteric sites. Either Mg^{2+} or Mn^{2+} supports guanylyl cyclase catalytic activity: Mg^{2+} supports basal and ligand-stimulated activity and is considered the physiological cofactor whereas Mn^{2+} supports ligand-independent activation (*12*).

The present studies examined the ability of Ca^{2+} to interact with and regulate purified sGC. The effects of Ca^{2+} on basal sGC immunopurified from bovine lung and that enzyme stimulated with ligands such as SNP, PPIX, and YC-1, employing Mg- or Mn-GTP as substrate, were investigated. The mechanisms by which Ca^{2+} inhibits sGC were explored by analyzing substrate kinetics. Similarly, the role of free Mg^{2+}, required for sGC activity, in mechanisms mediating Ca^{2+} inhibition was examined. Finally, the ability of purified sGC to directly bind $^{45}Ca^{2+}$ was explored. These studies suggest that sGC is a constitutive Ca^{2+} binding protein whose allosteric function is conditionally coupled to catalytic inhibition by ligand activation.

METHODS AND MATERIALS

Materials. Soluble GC purified from bovine lung (*13*) and YC-1 were obtained from Alexis Biochemical Corporation (San Diego, CA). EGTA, GTP, SNP, PPIX, acetic anhydride, triethylamine, and purified calmodulin were purchased from Sigma (St. Louis, MO). All other reagents were from Fisher Scientific (Pittsburgh, PA).

Guanylyl Cyclase Assays. Soluble GC was diluted according to the manufacturer with buffer containing 88 mM NaCl,

1 mM DTT, 0.5 mM EDTA, 25 mM Tris, pH 7.4, and 0.5 mg/mL BSA. Enzyme activity was determined employing Mg-GTP, Mn-GTP, or Ca-GTP as substrate, as described previously (*14*). Reactions (100 μL) contained 5 ng of purified sGC, 50 mM Tris (pH 7.4), 1 mM DTT, 0.5 mg/mL BSA, and various concentrations of Me-GTP substrate and free $MeCl_2$ (*13*). Some incubations contained activating ligands including 50 μM SNP (*15*), 200 μM YC-1 (*16*), or 100 μM PPIX (*17*). Also, some incubations contained specific concentrations of free Ca^{2+} and Mg^{2+} buffered with 100 μM EGTA, which were determined employing the Winmax computer program (http://www.stanford.edu/-cpatton/maxc.html). Incubations (37 °C) were initiated by the addition of enzyme, continued for various amounts of time, and terminated by adding 400 μL of 50 mM sodium acetate (pH 4.0) and boiling for 3 min. Enzyme activity was linear with respect to time and protein concentration under all conditions examined. Enzyme assays were performed in duplicate, and cGMP was quantified in each sample by radioimmunoassay in triplicate as described previously (*7*). Results are representative of at least three separate experiments. Analyses of enzyme kinetics were performed using *Prism* (GraphPad Software Inc., San Diego, CA) or Microsoft Excel (Redmond, WA). Statistical significance was determined using paired Student's *t* tests (two-tailed) employing Microsoft Excel (Redmond, WA).

Purity of sGC. sGC (1.25 μg), purified by immunoaffinity chromatography employing an antibody to the C-terminus of the β1 subunit (*13*), was analyzed by SDS−PAGE on a precast 8 × 10 cm 12.5% polyacrylamide gel (Owl, Portsmouth, NH) as described previously (*13*). The gel was stained with Gelcode Blue (Pierce Rockfort, IL).

$^{45}Ca^{2+}$ Overlay Analysis. $^{45}Ca^{2+}$ overlay was performed essentially as described (*18*). Nitrocellulose membranes were washed in buffer containing 10 mM imidazole-HCl, pH 6.8, 5 mM $MgCl_2$, and 60 mM KCl, and purified sGC (2.5 μg), purified calmodulin (4 μg; positive control), and BSA (10 μg; negative control) were applied using a dot-blot apparatus. Membranes were incubated in buffer containing 10 mM imidazole-HCl, pH 6.8, 5 mM $MgCl_2$, 60 mM KCl, and 10 μCi of $^{45}Ca^{2+}$/mL (5 μM), for 10 min, washed three times with 40% ethanol for 5 min, dried at 25 °C for 3 h, and analyzed by phosphorimager (18 h, 25 °C; Molecular Dynamics, Sunnyvale, CA). Subsequently, the same membranes were probed with anti-sGC antibody (Cayman, Ann Arbor, Michigan), and specific binding was visualized with the NovaRED substrate kit for peroxidase (Vector Laboratories Burlingame, CA).

RESULTS

Ca^{2+} Inhibits sGC Stimulated by SNP using Mg-GTP as the Substrate. Previous studies demonstrated that 250 μM Ca^{2+} inhibited SNP-stimulated sGC heterologously expressed in HEK 293 cells ~80% (*7*). In the present study, the effect of 250 μM Ca^{2+} on the activity of purified sGC was examined in the presence of 100 μM GTP, the physiological concentration of GTP (*19*−*21*). Ca^{2+} inhibited SNP-stimulated purified sGC ~80% (Figure 1A). In contrast, up to 1 mM Ca^{2+} had no effect on basal purified sGC (Figure 1A and data not shown). To examine whether Ca^{2+} inhibits sGC by preventing formation of NO from SNP or interaction of NO with the heme prosthetic group of the enzyme, sGC was stimulated by the NO-independent activators PPIX (100 μM) and YC-1 (200 μM). The activity of sGC stimulated by PPIX and YC-1 was inhibited ~70% by 250 μM Ca^{2+} (Figure 1A). To examine whether the insensitivity of basal sGC to Ca^{2+} reflected competition by excess free Mg^{2+}, the effects of Ca^{2+} on sGC were assessed in the absence of excess Mg^{2+} (Figure 1B). Basal sGC activity [7.98 ± 3.26 nmol of cGMP min^{-1} (mg of protein)$^{-1}$] was not significantly affected by 250 μM Ca^{2+} [7.41 ± 2.00 nmol of cGMP min^{-1} (mg of protein)$^{-1}$] while SNP-activated sGC was inhibited >90% (Figure 1B). Ca^{2+} (250 μM) did not significantly alter the V_{max} or K_m of basal sGC (Figure 1C, Table 1), whereas the V_{max} and K_m of SNP-stimulated sGC were significantly reduced ($p < 0.05$) (Figure 1D, Table 1).

Table 1: Kinetic Parameters of SGC Employing Various Metal Cations as Substrate Cofactor

				250 μM Ca^{2+}	
	Mn-GTP	Mg-GTP	Ca-GTP	Mn-GTP	Mg-GTP
	V_{max}[a] (nmol of cGMP min^{-1} (mg of protein)$^{-1}$)				
−SNP	503 ± 191	205 ± 11.0	31.0 ± 5.8	432 ± 13.0	229 ± 8.6
+SNP	1396 ± 211	5337 ± 907	42.0 ± 8.2	1265 ± 123	538 ± 206[b]
	K_m[a] (μM)				
−SNP	30.5 ± 14.9	212.7 ± 21.3	20.0 ± 2.5	30.0 ± 9.5	261.6 ± 60.7
+SNP	13.5 ± 4.2	61.3 ± 5.6	3.0 ± 1.0	14.5 ± 6.0	8.3 ± 1.2[b]

[a] K_m and V_{max} values are extracted from linear regression analyses of double reciprocal plots of Mg-GTP, Mn-GTP, and Ca-GTP activity of sGC in the absence or presence of 50 μM SNP. Values are means ± SEM of K_m and V_{max} values of three experiments performed in duplicate. Data are presented in Figures 1, 2, and 3. [b] $p < 0.05$ with respect to control (no added Ca^{2+}) employing the paired Student's *t* test (two-tailed).

Ca^{2+} Does Not Inhibit sGC when Mn-GTP is the Substrate. Employing Mn^{2+} as the cation cofactor, basal sGC activity was higher as compared to that in the presence of Mg^{2+}, reflecting the ability of the former cation to activate nucleotide cyclases in a ligand-independent fashion (Figure 2A) (*12*). Indeed, in the presence of Mn^{2+}, activation by ligands such as SNP, PPIX, and YC-1 was lower, as a percent of basal activity, than that obtained employing Mg^{2+} (compare Figures 1A and 2A) as described previously (*4*, *12*, *13*, *15*). Employing Mn^{2+} as the cation cofactor, Ca^{2+} (up to 1 mM) did not inhibit basal or ligand-stimulated sGC (Figure 2A and data not shown). Indeed, Ca^{2+} did not alter the V_{max} or K_m of sGC when Mn^{2+} served as the cation cofactor (Figure 2B,C; Table 1). Preservation of ligand stimulation in the presence of Ca^{2+} employing Mn^{2+} as the substrate cofactor eliminates the possibility that Ca^{2+} inhibits sGC by dissociating the heme prosthetic group, required for ligand activation.

Ca-GTP Serves as a Substrate for, but Does Not Support Ligand Activation of, sGC. Ca^{2+} could inhibit sGC, in part, by forming a complex with GTP and serving as a substrate with high affinity but poor catalytic characteristics that competes with Mg-GTP. Indeed, when Ca-GTP served as the substrate for sGC, V_{max} was significantly lower than that obtained employing other Me-GTP substrates, whereas the affinity of the enzyme for Ca-GTP was significantly higher than that for other Me-GTP complexes (Figure 3, Table 1). These observations are in close agreement with previous studies demonstrating that Ca^{2+} serves as a poor cation cofactor for sGC (*22*, *23*). Alternatively, Ca^{2+} could inhibit

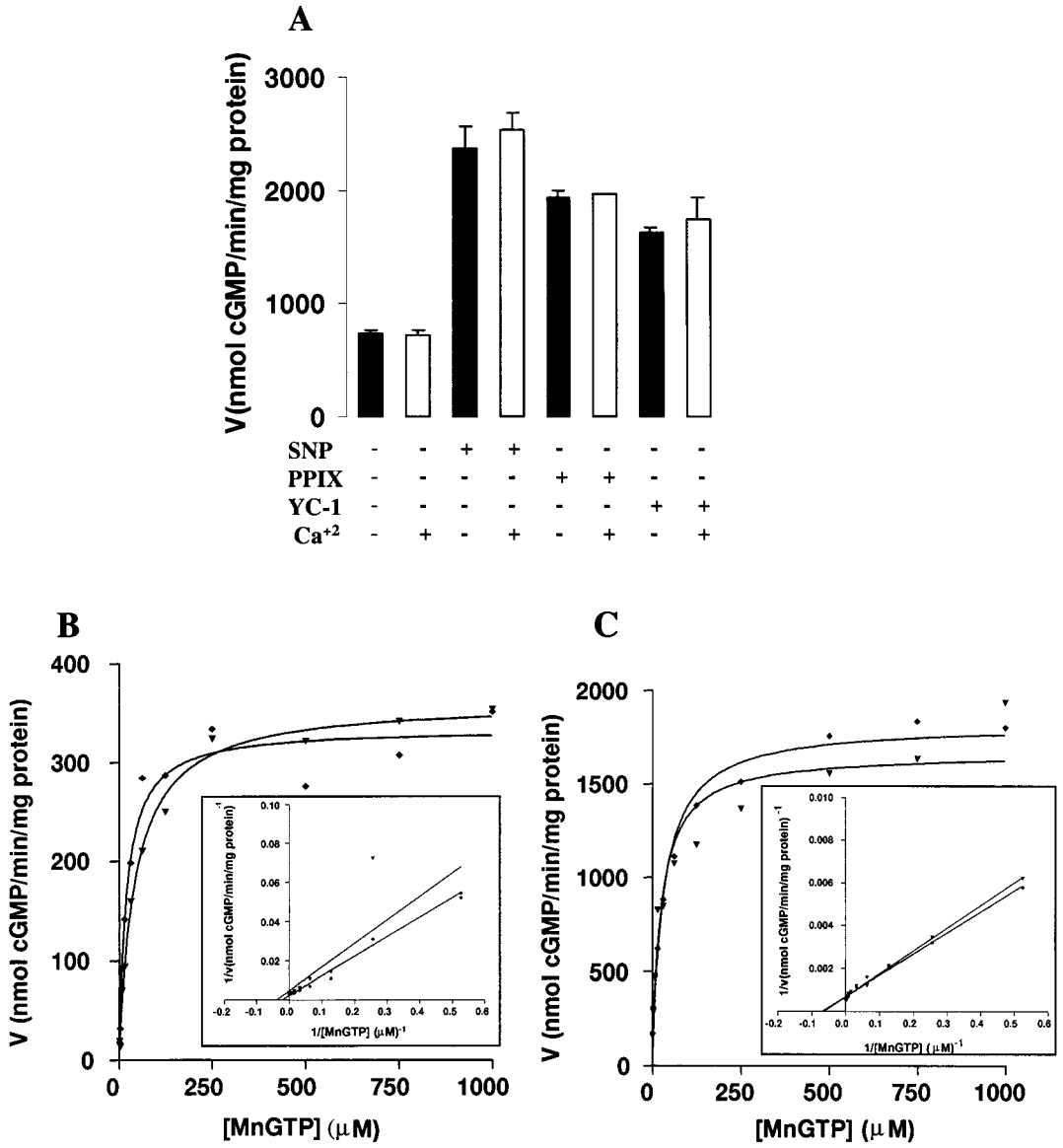

FIGURE 2: Ca^{2+} inhibition of purified sGC employing Mn-GTP as the substrate. The activity of purified sGC (5 ng) was quantified as described in Methods in incubations (37 °C, 10 min) containing (A) 100 μM Mn-GTP, excess 3 mM Mn^{2+} and, where indicated, 50 μM SNP, 100 μM PPIX, 200 μM YC-1, or 250 μM Ca^{2+}; (B) increasing concentrations of Mn-GTP (10−1000 μM) 3 mM excess Mn^{2+} and 0 μM (▼) or 250 μM (◆) Ca^{2+}; (C) increasing concentrations of Mn-GTP (10−1000 μM), 3 mM excess Mn^{2+}, 50 μM SNP, and 0 μM (▼) or 250 μM (◆) Ca^{2+}. These results are representative of ≥3 experiments performed in duplicate. Insets: linear analysis of double-reciprocal plots used to estimate V_{max} and K_m values presented in Table 1.

sGC by competing with free Mg^{2+} for the positive allosteric Me-binding site required for ligand activation. Of significance, Ca^{2+} in excess of substrate did not support SNP activation of sGC, demonstrating its inactivity at the positive allosteric Me-binding site (Figure 3, Table 1).

High and Low Affinity Sites on sGC Mediate Inhibition by Ca^{2+}. The concentration−response relationship of Ca^{2+} inhibition of SNP-activated sGC revealed the presence of two regulatory sites with high (10^{-7} M) and low (10^{-5} M) affinity for Ca^{2+} (Figure 4). To examine whether inhibition mediated by one or both sites reflected competition between Ca^{2+} and Mg^{2+} for key Me-binding sites required for ligand activation, the concentration−response relationship of Ca^{2+} inhibition of sGC was determined in the presence of 300 μM Mg^{2+}, which is the physiological intracellular concentration of that cation, and 3 mM Mg^{2+} (*24*−*26*). Increasing Mg^{2+} from 300 μM to 3 mM did not significantly alter the K_i of Ca^{2+} at the high affinity site, although it reduced the maximum inhibition by that cation (Figure 4, Table 2). In contrast, increasing the concentration of Mg^{2+} from 300 μM to 3 mM shifted the concentration−response relationship of the low affinity Ca^{2+} binding site to the right with an associated increase in the apparent K_i of this site (Figure 4, Table 2).

Ca^{2+} Inhibition Mediated by High and Low Affinity Sites Reflect Different Kinetic Mechanisms. Because Ca^{2+} can serve as a substrate cofactor for sGC (Figure 3, Table 1), concentrations of Mg^{2+} (3 mM) that minimized formation of Ca-GTP complexes were employed. Under these conditions, the concentration of Mg^{2+}-GTP was >1000-fold greater than that of Ca^{2+}-GTP at all concentrations of Mg^{2+}, Ca^{2+}, and GTP employed except at 100 and 250 μM Ca^{2+}, where Mg^{2+}-GTP was >100-fold and >40-fold greater than Ca^{2+}-GTP, respectively. The effect mediated by the high affinity site on enzyme kinetics was examined employing 500 nM Ca^{2+} (Figure 5). These analyses revealed that Ca^{2+}

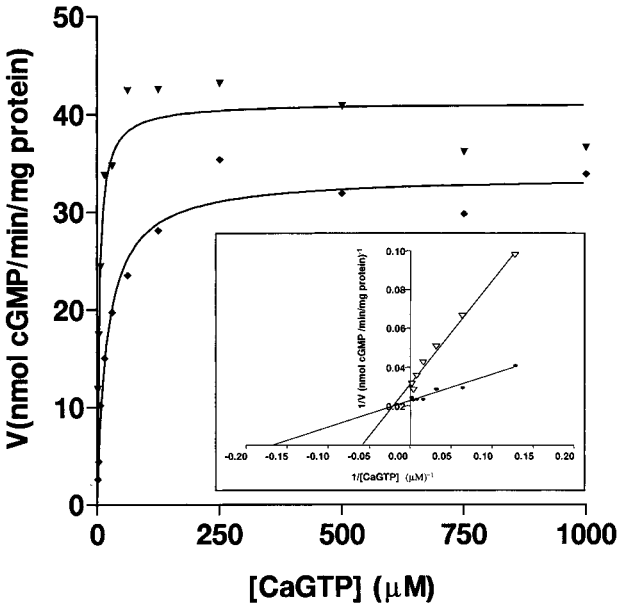

FIGURE 3: sGC quantified employing Ca-GTP as the substrate. The activity of purified sGC (5 ng) was quantified in incubations (37 °C, 10 min) containing increasing concentrations of Ca-GTP (10−1000 μM), 3 mM excess Ca^{2+}, and 0 μM (◆) or 50 μM (▼) SNP. Results are representative of ≥3 experiments performed in duplicate. Inset: linear analysis of double-reciprocal plots used to estimate V_{max} and K_m values presented in Table 1.

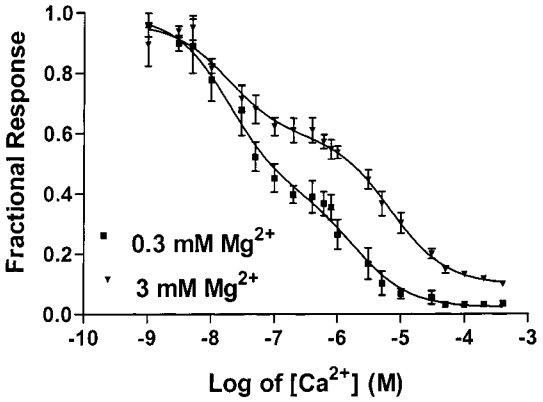

FIGURE 4: Concentration-response relationship of Ca^{2+} inhibition of sGC. The activity of purified sGC (5 ng) was quantified in incubations (37 °C, 5 min) containing 50 μM SNP, increasing Ca^{2+} concentrations (10^{-9}−10^{-3} M), 100 μM Mg-GTP, and 300 μM (■), or 3000 μM (▼) excess Mg^{2+}. The maximal velocity (fractional velocity = 1) reflected the velocity determined in the absence of Ca^{2+}. Values are means ± SEM of ≥3 experiments performed in duplicate. Analyses of these data are presented in Table 2.

inhibition mediated by the high affinity site was associated with a significant decrease in V_{max} without an alteration in the K_m of SNP-activated sGC, consistent with a noncompetitive mechanism (Table 3). In contrast, Ca^{2+} inhibition mediated by the low affinity site, examined employing >10 μM Ca^{2+}, was associated with a significant decrease in V_{max} and K_m ($p < 0.05$) with parallel double reciprocal plots characteristic of an uncompetitive mechanism (Figure 5, Table 3).

Ca^{2+} Competes with Mg^{2+} at the Low, but not High, Affinity Site on sGC. Studies described above demonstrate that Ca^{2+} does not support SNP-activation of sGC, suggesting that it may serve as an antagonist at the free metal binding site required for ligand activation (see Figure 3). Similarly,

Table 2: K_i of Ca^{2+} Inhibition of SGC and Hill Coefficient Related to Each Ca^{2+} Binding Site

	K_i[a]		Hill coefficent[b]	
excess Mg^{2+} (μM)	high affinity (μM)	low affinity (μM)	high affinity	low affinity
300	0.17 ± 0.04	28.6 ± 13.5	1.4 ± 0.42	1.46 ± 0.42
3000	0.15 ± 0.04	98.5 ± 24.7[c]	1.25 ± 0.52	0.93 ± 0.04

[a] Nonlinear regression analyses were performed employing one- or two-component models (*Prism*, GraphPad Software Inc., San Diego, CA) for each of the Mg^{2+} concentrations employed, to estimate the K_i values (*37*). Goodness of fit was quantified by the least-squares method (F-test) and was determined to be best suited to a two-component model ($p < 0.0001$). Values are means ± SEM of effective concentrations of Ca^{2+} yielding 50% of the response for high and low affinity sites, respectively, in four experiments performed in duplicate. Experiments were performed employing buffered calcium solutions. Data are presented in Figure 4. [b] Hill coefficients for each site were extracted from nonlinear regression analyses employing a sigmoidal dose−response curve and four-parameter logistic analysis (*Prism*, GraphPad Software Inc., San Diego, CA). Values are means ± SEM of ≥ 3 experiments performed in duplicate. [c] A significant difference ($p < 0.05$) with respect to K_i for low affinity sites in the presence of 300 μM Mg^{2+} as determined by a paired Student's *t* test (two tailed).

increased Mg^{2+} shifted the concentration−response relationship to Ca^{2+} of the low affinity site to the right, consistent with an interaction of those cations at that site (see Figure 4). The interaction of those divalent cations was analyzed further by examining the effect of Ca^{2+} at low and high affinity sites on the requirement for free Mg^{2+} to support maximum activation of sGC by SNP. Free Mg^{2+}, up to a maximum of ~4 mM, increased sGC activity stimulated by SNP in a concentration-dependent fashion while higher concentrations (7 and 10 mM) were inhibitory (Figure 6). Ca^{2+} at a concentration that inhibited at the high affinity site only (500 nM), decreased the activity without shifting the concentration−response relationship to Mg^{2+} to the right or significantly altering the K_a for that cation. However, 100 μM and 250 μM Ca^{2+}, which bind both high and low affinity sites, decreased the activity and shifted the concentration−response relationship to Mg^{2+} to the right with an associated significant increase in the K_a ($p < 0.05$) for that cation (Figure 6, Table 4). These data are consistent with a mechanism in which Ca^{2+} inhibits SNP-activated sGC, in part, by competitively antagonizing Mg^{2+} binding at the low affinity site, which is the positive allosteric metal binding site required for ligand activation.

sGC is a Ca^{2+} Binding Protein. SDS−PAGE demonstrated that preparations of sGC purified by immunoaffinity chromatography were composed of 73 (α) and 70 (β) kDa subunits (Figure 7). Densitometric analysis of these preparations following SDS−PAGE revealed that >95% of their composition was α and β subunits. These observations are identical to those reported previously for purification of this enzyme by immunoaffinity chromatography employing the same antibody (*13*). Purified sGC spotted on nitrocellulose specifically bound $^{45}Ca^{2+}$ when these blots were incubated in Ca^{2+}- and SNP-free buffer containing 5 mM Mg^{2+} to which was added 5 μM $^{45}Ca^{2+}$. Similarly, purified calmodulin (positive control) but not BSA (negative control) also bound $^{45}Ca^{2+}$ when spotted on nitrocellulose adjacent to purified sGC. The presence of sGC on the nitrocellulose was confirmed by Western analysis employing anti-sGC antibody. These data demonstrate that Ca^{2+} binds to sGC in the

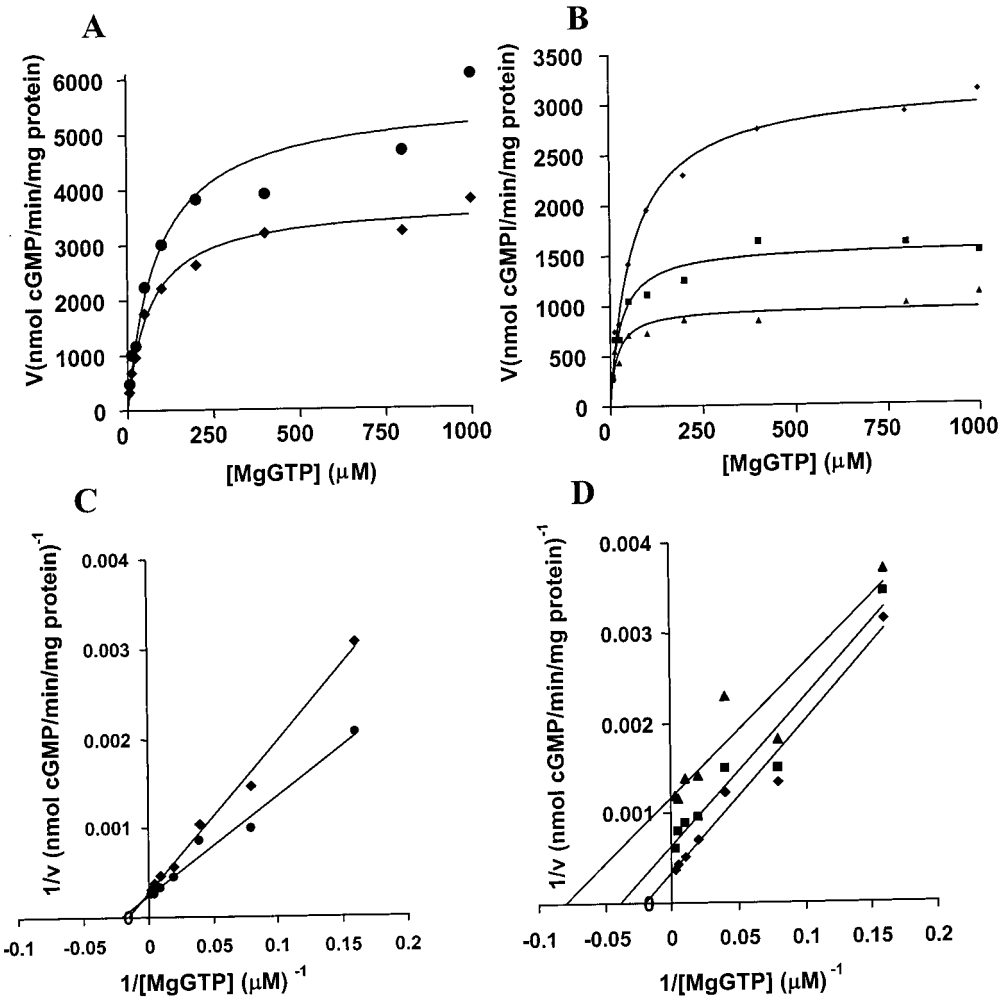

FIGURE 5: Effects of Ca^{2+} at high and low affinity sites on the substrate kinetics of purified sGC. The activity of purified sGC (5 ng) was quantified in incubations (37 °C, 5 min) containing 50 μM SNP, increasing concentrations of Mg-GTP (10−1000 μM), 3 mM excess Mg^{2+} and (A) 0 nM (●) and 500 nM (◆) Ca^{2+}; (B) 10 μM (◆), 100 μM (■), and 250 μM (▲) Ca^{2+}. Data presented in Michaelis plots in (A) and (B) were subjected to double reciprocal analysis, presented in (C) and (D), respectively. Results are representative of ≥3 experiments performed in duplicate. Analyses of these data are presented in Table 3.

Table 3: Kinetic Parameters of High and Low Affinity Inhibitory Sites of SGC

μM Ca^{2+}	V_{max}[a] (nmol of cGMP min^{-1} (mg of protein)$^{-1}$)	K_m[a] (μM)
0	4069 ± 370	75.2 ± 18.2
0.5	2835 ± 565[b]	65.7 ± 5.7
10	2308 ± 452[b]	61.6 ± 13.4
100	1311 ± 227[b]	39.4 ± 17.9[b]
250	737 ± 114[b]	22.5 ± 10.0[b]

[a] Values are means ± SEM of V_{max} and K_m values extracted from linear regression analyses of three experiments performed in duplicate. Experiments were performed employing buffered calcium solutions. Data are presented in Figure 5. [b] $p < 0.05$ with respect to control (no added Ca^{2+}) determined by paired Student's t test (two tailed).

unliganded state (absence of SNP) specifically at the high affinity site ($K_i \sim 10^{-7}$ M), which does not compete directly with Mg^{2+} ($^{45}Ca^{2+}$ binding in the presence of >1000-fold excess of Mg^{2+}).

DISCUSSION

Coordination between cGMP- and Ca^{2+}-mediated pathways, which in many physiological systems regulate opposing processes, is reflected in the reciprocal regulation of the intracellular concentrations of these signaling molecules. Mechanisms by which $[cGMP]_i$ regulates $[Ca^{2+}]_i$ have been described in hepatocytes, neuronal cells, VSMC, and retinal photoreceptor cells and include alterations in Ca^{2+} influx and efflux across the plasma membrane and release and uptake into intracellular storage pools (*4*, *27*−*29*). However, mechanisms by which $[Ca^{2+}]_i$ regulates $[cGMP]_i$ have not been completely defined. The present study demonstrates that Ca^{2+} allosterically inhibits sGC, purified to apparent homogeneity, in a concentration-dependent and saturable fashion. Ca^{2+} directly inhibits purified sGC in the physiological range of concentrations of that cation, without the involvement of a regulatory cofactor.

Ca^{2+} inhibited sGC only when activated by ligands such as SNP, suggesting that inhibition might involve interruption of the molecular mechanism by which ligands activate sGC. SNP activates sGC by generating NO, which binds to a heme prosthetic group in the amino terminal domain of sGC (*4*). Association of NO with the Fe^{3+} center of heme is coupled to activation of the catalytic domain of sGC, increasing the V_{max} of that enzyme (*4*). Ca^{2+} might inhibit SNP activation of sGC by preventing the formation of the proximal activating ligand NO from SNP or interrupting NO−heme interaction on sGC. However, PPIX mimics the liganded

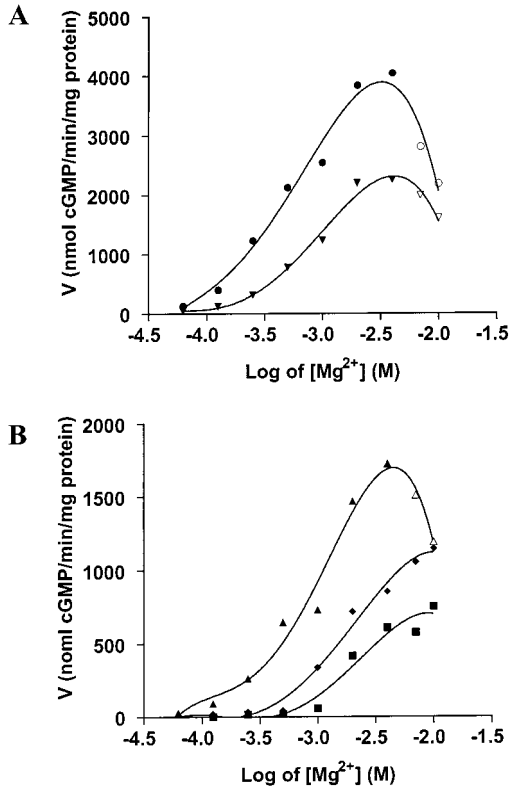

FIGURE 6: Effects of Ca^{2+} on the concentration-dependence of sGC activation by Mg^{2+}. The activity of purified sGC (5 ng) was quantified in incubations (37 °C, 5 min) containing 50 μM SNP, 100 μM Mg-GTP, increasing concentrations of excess free Mg^{2+} (100−10,000 μM) and (A) 0 nM (●) and 500 nM Ca^{2+} (▼) or (B) 10 μM (▲), 100 μM (◆), or 250 μM (■) Ca^{2+}. Results are representative of ≥3 experiments performed in duplicate. Analyses of these data are presented in Table 4.

Table 4: Effect of Free Mg^{2+}on Ca^{2+} Inhibition of sGC[a]

μM Ca^{2+}	specific activity (nmol of cGMP min^{-1} (mg of protein)$^{-1}$)	K_a (mM)
0	6066 ± 1177	0.26 ± 0.20
0.5	3604 ± 730[b]	0.39 ± 0.30
10	2591 ± 328[b]	0.65 ± 0.50
100	1464 ± 192[b]	1.20 ± 0.30[b]
250	897 ± 156[b]	1.50 ± 0.30[b]

[a] Values are means ± SEM of ≥3 experiments performed in duplicate. K_a values were extracted from nonlinear regression analyses employing a sigmoidal dose−response curve and four-parameter logistic analysis (*Prism*, GraphPad Software Inc., San Diego, CA) of the Mg^{2+} dose responses. Because $[Mg^{2+}]$ ≥7 mM was inhibitory when 0, 500 nM, and 10 μM Ca^{2+} was employed, only values related to $[Mg^{2+}]$ < 7 mM were used to calculate specific activity and K_a at these concentrations of Ca^{2+}. Experiments were performed employing buffered calcium solutions. Hill coefficients for the effects of free Mg^{2+}on sGC were 0 μM Ca^{2+}, 2.09 ± 1.64; 0.5 μM Ca^{2+}, 4.31 ± 2.16; 10 μM Ca^{2+}, 1.57 ± 0.51; 100 μM Ca^{2+}, 2.81± 0.79; 250 μM Ca^{2+}, 3.22 ± 1.00. Data are presented in Figure 6. [b] $p < 0.05$ with respect to control (no added Ca^{2+}) determined by paired Student's *t* test (two tailed).

heme−NO complex and directly activates sGC in the absence of NO (*17*), whereas YC-1 activates sGC by a mechanism that does not involve interaction with, but is dependent upon heme (*30*, *31*). That Ca^{2+} inhibited sGC activated by SNP, PPIX, and YC-1 demonstrated that inhibition does not reflect prevention of NO formation or its interaction with sGC, since neither PPIX nor YC-1 activate that enzyme in an NO-dependent fashion. Similarly, inhibition might reflect displacement of heme from sGC by Ca^{2+}, rendering that enzyme incompetent to respond to NO, PPIX, or YC-1. Of significance, Ca^{2+} had no effect on sGC activated by SNP, PPIX, or YC-1 when Mn^{2+} served as the cation cofactor, suggesting that Ca^{2+} does not displace heme from sGC. It should be noted that these data do not eliminate the possibility that Ca^{2+} disrupts the association between heme and the enzyme when Mg^{2+}, but not Mn^{2+}, serves as the cation cofactor.

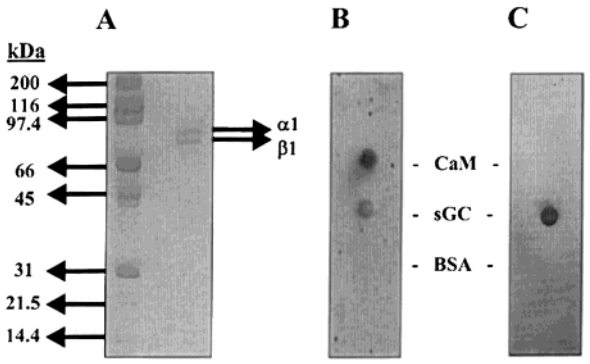

FIGURE 7: Purified sGC specifically binds $^{45}Ca^{2+}$. (A) Purified sGC (1.25 μg) was subjected to SDS−PAGE on a 12.5% polyacrylamide gel and stained with Gelcode Blue and the two subunits α1 (73 kDa) and β1 (70 kDa) were detected. (B) Calmodulin (4 μg), purified sGC (2.5 μg), and BSA (10 μg) were applied to a nitrocellulose membrane and binding of $^{45}Ca^{2+}$ was assessed as described in Methods. (C) The nitrocellulose membrane in (B) was probed with anti-sGC antibody as described in Methods. Data are representative of three experiments.

The concentration−response relationship for Ca^{2+} inhibition of SNP-activated sGC revealed discreet binding sites with high or low affinity for Ca^{2+}. High affinity sites exhibit a K_i ($\sim 10^{-7}$ M) compatible with physiological $[Ca^{2+}]_i$, whereas supraphysiological $[Ca^{2+}]_i$ inhibit sGC at low affinity sites ($K_i \sim 10^{-5}$ M). High and low affinity Ca^{2+} binding sites may permit cells with large variations in $[Ca^{2+}]_i$ to allosterically regulate sGC and, consequently, $[cGMP]_i$ over a wide dynamic range of cation concentrations. For example, in the relaxed state VSMCs exhibit $[Ca^{2+}]_i < 10^{-7}$ M, whereas they exhibit $[Ca^{2+}]_i \geq 10^{-6}$ M in the contracted state (*32*). In these cells, which are constitutively exposed to NO produced by the endothelium, low $[Ca^{2+}]_i$, characteristic of the relaxed state, regulates sGC by binding to high affinity sites, limiting accumulation of $[cGMP]_i$. When these cells are exposed to a contractile stimulus, $[Ca^{2+}]_i$ increases and may interact with high and low affinity sites, imposing even greater limitations upon the accumulation of $[cGMP]_i$ during contraction. Furthermore, proximity to calcium channels, whose local concentrations of $[Ca^{2+}]_i$ approach 10^{-4} M, would saturate low affinity sites on sGC, completely inhibiting cGMP production (*33*).

Examination of the relationship between the concentration-dependence of Ca^{2+}, substrate, and free Mg^{2+} suggests specific distinct mechanisms mediate inhibition of sGC. Analysis of substrate kinetics revealed that Ca^{2+} inhibition at the high affinity site was mediated by a noncompetitive mechanism (see Figure 5). Also, increasing $[Mg^{2+}]$ from 300 μM, which is within the physiological range of free $[Mg^{2+}]_i$, to 3 mM did not significantly change the K_i value of the high affinity site, suggesting that these cations do not compete at that site (see Figure 4). Similarly, Ca^{2+} at concentrations that specifically interact with high affinity sites

did not alter the K_a for binding of Mg^{2+} to sGC, supporting the suggestion that these cations do not interact at that site (see Figure 6). Therefore, the high affinity site for Ca^{2+} is distinct from the two known metal binding sites (catalytic site and free metal binding site) for guanylyl cyclases. However, it is noteworthy that free $[Mg^{2+}] \geq 7$ mM directly inhibited NO-stimulated sGC (see Figure 6) (*11*). These data support a model in which the high affinity site represents a novel divalent cation binding site that mediates allosteric inhibition of sGC with a rank order of potency: $Ca^{2+} \gg Mg^{2+}$.

In contrast, analysis of substrate kinetics revealed that Ca^{2+} inhibition at the low affinity site was mediated by an uncompetitive mechanism (see Figure 5). That increasing $[Ca^{2+}]$ decreases V_{max} in association with a decrease in K_m, apparently increasing the affinity of the enzyme for its substrate, supports the suggestion that calcium inhibition of sGC at the low affinity site is mediated by an allosteric mechanism. Increasing $[Mg^{2+}]$ from 300 μM to 3 mM significantly increased the K_i value of, the low affinity site, suggesting that these cations compete at that site (see Figure 4). Similarly, Ca^{2+} at concentrations that interact with high and low affinity sites shifted the concentration-dependence of enzyme activation by free Mg^{2+} to the right, producing an increase in the K_a of that cation, supporting the suggestion that Ca^{2+} and Mg^{2+} compete at low affinity site (see Figure 6). In this regard, it is noteworthy that Ca^{2+}, when employed as the sole cation, did not support ligand activation, suggesting that this cation is ineffective at the positive allosteric cation binding site required for ligand activation (see Table 1). Taken together, these data support a model in which the low affinity site is identical to the positive allosteric cation binding site required for ligand activation. Ca^{2+} inhibits sGC at that site by serving as a competitive antagonist with a higher affinity than Mg^{2+}, but an inability to activate this site.

In the present study, Ca^{2+} inhibited ligand-stimulated, but not basal, sGC, as observed previously in other systems. Thus, L-ascorbate inhibited sGC purified from bovine lung stimulated by NO-dependent or -independent ligands, without altering basal activity (*34*). Also, dephosphorylation of the β subunit of bovine adrenal sGC inhibited SNP-stimulated, but not basal enzyme activity (*35*). In addition, sGC purified from human cerebral cortex was selectively inhibited by its reaction products, cGMP and pyrophosphate, in the activated as compared to the basal state (*36*). In the study described herein, dependence on ligand activation of Ca^{2+} inhibition at the low affinity site reflects the specific role of the positive allosteric cation site in ligand activation of sGC. However, ligand activation may unmask novel high affinity binding sites that mediate inhibition or may couple constitutive high affinity sites to inhibition of the catalytic domain. Indeed, $^{45}Ca^{2+}$ specifically bound to sGC in the basal state at concentrations compatible with the high affinity site in the presence of >1000-fold excess of free Mg^{2+} (see Figure 7), supporting a model in which ligand activation couples constitutive high affinity Ca^{2+} binding sites to allosteric inhibition of the catalytic domain.

High and low affinity Ca^{2+} binding sites also mediate allosteric inhibition of mammalian AC type V and VI (*37*−*41*). Indeed, Ca^{2+} inhibition of AC at high and low affinity sites exhibits kinetic characteristics that are nearly identical to those reported herein for inhibition of sGC (*42*, *43*). Ca^{2+} inhibits AC by interacting directly with a specific sequence in the enzyme that is not homologous to previously defined Ca^{2+} binding motifs (*44*). Similarly, the present study suggests that Ca^{2+} inhibits sGC by direct interaction with that protein, in which there are no defined Ca^{2+} binding motifs. These data suggest that allosteric inhibition by direct interaction of Ca^{2+} with nucleotide cyclases may be a generalized mechanism coordinating the reciprocal regulation of intracellular concentrations of cyclic nucleotides and Ca^{2+} that mediate opposing physiological processes.

The mechanism by which Mn^{2+} confers resistance to inhibition by Ca^{2+} remains unclear. Mn^{2+} activates nucleotide cyclases in a ligand-independent fashion by an undefined mechanism (*4*, *12*). In addition, Mn^{2+} supports activation of sGC by ligands (see Figure 2), suggesting that it binds to and activates the positive allosteric divalent cation binding site required for ligand activation. The resistance of Mn^{2+}-activated sGC to Ca^{2+} inhibition may reflect a differential affinity of cations for high and low affinity negative allosteric sites, in which the rank order of potency is $Mn^{2+} \gg Ca^{2+}$. Alternatively, binding of Mn^{2+} to sGC could regulate negative allosteric sites mediating Ca^{2+} inhibition. These alternate mechanisms will specifically be examined in ongoing studies defining the binding characteristics of $^{45}Ca^{2+}$ to purified sGC.

Coordinated regulation of $[Ca^{2+}]_i$ and $[cGMP]_i$ described previously in retinal photoreceptor cells is mediated, in part, by GCAPs, tissue-specific Ca^{2+}-binding proteins that stimulate retinal membrane-bound GC in the presence of low $[Ca^{2+}]_i$ (*45*, *46*). In those cells, cGMP and Ca^{2+} regulate opposing limbs of the phototransduction cascade. Ca^{2+} flows into these cells through cyclic nucleotide-gated channels that are open in the dark but closed in the light (*4*). Light activates a cGMP-specific phosphodiesterase and the resultant hydrolysis reduces $[cGMP]_i$, closes cyclic nucleotide-gated channels, and reduces $[Ca^{2+}]_i$. This change in $[Ca^{2+}]_i$ activates GCAPs and stimulates GC. GCAPs behave as sensitive Ca^{2+} switches for the coordinated regulation of $[cGMP]_i$ by retinal membrane-bound GC with a K_i for that cation in the high nanomolar range (*47*−*49*). The present study demonstrates that sGC also behaves as a sensitive Ca^{2+} switch with a broad dynamic response range and an affinity for that cation in the high nanomolar range. These data suggest that there are multiple mechanisms by which $[Ca^{2+}]_i$ regulates $[cGMP]_i$ involving tissue-specific Ca^{2+}-sensitive accessory proteins and direct regulation of GCs.

In summary, the present study demonstrates that purified sGC is a constitutive Ca^{2+} binding protein whose function is conditionally coupled to allosteric inhibition of the catalytic domain by ligand activation. Ca^{2+} regulates sGC by binding to discrete high and low affinity sites that allosterically inhibit sGC by distinct mechanisms. High (nanomolar) affinity sites are unique cation binding sites that are coupled to allosteric inhibition of the catalytic domain by ligand activation of sGC. In contrast, low (micromolar) affinity sites are identical to cation binding sites required for ligand activation of sGC and inhibition reflects antagonism of Mg^{2+} binding by Ca^{2+}, which is ineffective in supporting enzyme activation at this site. The combination of high and low affinity binding sites permits sGC and, consequently, $[cGMP]_i$ to be regulated over a wide dynamic range (10^{-9}−10^{-4} M) of $[Ca^{2+}]_i$ and with

high (nanomolar) sensitivity. This appears to be a mechanism that could contribute to the regulation of $[cGMP]_i$ by $[Ca^{2+}]_i$ in all cells expressing sGC. Indeed, it is likely to be one mechanism contributing to the coordinated regulation of $[cGMP]_i$ and $[Ca^{2+}]_i$ mediating opposing processes in many systems including VSMCs, retinal photoreceptors, platelets, pancreatic acinar cells, and neurons.

ACKNOWLEDGMENT

The authors thank Dr. Kenneth P. Chepenik for critical review of the manuscript.

REFERENCES

1. Buechler, W. A., Nakane, M., and Murad, F. (1991) *Biochem. Biophys. Res. Comm. 174*, 351−7.
2. Harteneck, C., Koesling, D., Soling, A., Schultz, G., and Bohme, E. (1990) *FEBS Lett. 272*, 221−3.
3. Kamisaki, Y., Saheki, S., Nakane, M., Palmieri, J. A., Kuno, T., Chang, B. Y., Waldman, S. A., and Murad, F. (1986) *J. Biol. Chem. 261*, 7236−41.
4. Lucas, K. A., Pitari, G. M., Kazerounian, S., Ruiz-Stewart, I., Park, J., Schulz, S., Chepenik, K. P., and Waldman, S. A. (2000) *Pharmacol. Rev. 52*, 375−414.
5. Kamm, K. E., and Stull, J. T. (1989) *Annu. Rev. Physiol. 51*, 299−313.
6. Peach, M. J., Singer, H. A., and Loeb, A. L. (1985) *Biochem. Pharmacol. 34*, 1867−74.
7. Parkinson, S. J., Jovanovic, A., Jovanovic, S., Wagner, F., Terzic, A., and Waldman, S. A. (1999) *Biochemistry 38*, 6441−8.
8. Andric, S. A., Kostic, T. S., Tomic, M., Koshimizu, T., and Stojilkovic, S. S. (2001) *J. Biol. Chem. 276*, 844−9.
9. Gukovskaya, A. S., and Pandol, S. J. (1995) *Am. J. Physiol. 268*, G900−7.
10. Liu, Y., Ruoho, A. E., Rao, V. D., and Hurley, J. H. (1997) *Proc. Natl. Acad. Sci. U.S.A. 94*, 13414−9.
11. Kimura, H., Mittal, C. K., and Murad, F. (1976) *J. Biol. Chem. 251*, 7769−73.
12. Waldman, S. A., and Murad, F. (1987) *Pharmacol. Rev. 39*, 163−96.
13. Humbert, P., Niroomand, F., Fischer, G., Mayer, B., Koesling, D., Hinsch, K. D., Gausepohl, H., Frank, R., Schultz, G., and Bohme, E. (1990) *Eur. J. Biochem. 190*, 273−8.
14. Waldman, S. A., O'Hanley, P., Falkow, S., Schoolnik, G., and Murad, F. (1984) *J. Infect. Dis. 149*, 83−9.
15. Gerzer, R., Hofmann, F., and Schultz, G. (1981) *Eur. J. Biochem. 116*, 479−86.
16. Friebe, A., and Koesling, D. (1998) *Molec. Pharmacol. 53*, 123−7.
17. Ignarro, L. J., Wood, K. S., and Wolin, M. S. (1982) *Proc. Natl. Acad. Sci. U.S.A. 79*, 2870−3.
18. Maruyama, K., Mikawa, T., and Ebashi, S. (1984) *J. Biochem. 95*, 511−519.
19. Bourne, H. R., Sanders, D. A., and McCormick, F. (1991) *Nature 349*, 117−27.
20. Hatakeyama, K., Harada, T., and Kagamiyama, H. (1992) *J. Biol. Chem. 267*, 20734−9.
21. Breitwieser, G. E., and Szabo, G. (1988) *J. Gen. Physiol. 91*, 469−93.
22. Garbers, D. L., and Hardman, J. G. (1975) *J. Biol. Chem. 250*, 2482−6.
23. Levine, S. N., Steiner, A. L., Earp, H. S., and Meissner, G. (1979) *Biochim. Biophys. Acta 566*, 171−82.
24. Jelicks, L. A., and Gupta, R. K. (1990) *J. Biol. Chem. 265*, 1394−400.
25. Quamme, G. A. (1993) *Am. J. Physiol. 264*, G383−9.
26. Schachter, M., Gallagher, K. L., and Sever, P. S. (1990) *Biochim. Biophys. Acta 1035*, 378−80.
27. Patel, S., Robb-Gaspers, L. D., Stellato, K. A., Shon, M., and Thomas, A. P. (1999) *Nat. Cell Biol. 1*, 467−71.
28. Yermolaieva, O., Brot, N., Weissbach, H., Heinemann, S. H., and Hoshi, T. (2000) *Proc. Natl. Acad. Sci. U.S.A. 97*, 448−53.
29. Willmott, N. J., Wong, K., and Strong, A. J. (2000) *J. Neurosci. 20*, 1767−79.
30. Friebe, A., Russwurm, M., Mergia, E., and Koesling, D. (1999) *Biochemistry 38*, 15253−7.
31. Kharitonov, V. G., Sharma, V. S., Magde, D., and Koesling, D. (1999) *Biochemistry 38*, 10699−706.
32. Capponi, A. M., Lew, P. D., and Vallotton, M. B. (1986) *J. Cardiovasc. Pharmacol. 8 Suppl 8*, S136−8.
33. Matthews, G. (1996) *Annu. Rev. Neurosci. 19*, 219−33.
34. Schrammel, A., Koesling, D., Schmidt, K., and Mayer, B. (2000) *Cardiovasc. Res. 47*, 602−8.
35. Ferrero, R., Rodriguez-Pascual, F., Miras-Portugal, M. T., and Torres, M. (2000) *J. Neurochem. 75*, 2029−39.
36. Lee, Y., Martin, E., and Murad, F. (2000) *Proc. Natl. Acad. Sci. U.S.A. 97*, 10763−10768.
37. Guillou, J. L., Nakata, H., and Cooper, D. M. (1999) *J. Biol. Chem. 274*, 35539−45.
38. Boyajian, C. L., Garritsen, A., and Cooper, D. M. (1991) *J. Biol. Chem. 266*, 4995−5003.
39. Cooper, D. M., Karpen, J. W., Fagan, K. A., and Mons, N. E. (1998) *Adv. Second Messenger Phosphoprotein Res. 32*, 23−51.
40. Giannattasio, G., Bianchi, R., Spada, A., and Vallar, L. (1987) *Endocrinology 120*, 2611−9.
41. Piascik, M. T., Addison, B., and Babich, M. (1985) *Archives of Biochemistry and Biophysics 241*, 28−35.
42. Oldham, S. B., Rude, R. K., Molloy, C. T., and Lipson, L. G. (1984) *Endocrinology 115*, 1883−90.
43. Lasker, R. D., Downs, R. W. J., and Aurbach, G. D. (1982) *Arch. Biochem. Biophys. 216*, 345−55.
44. Scholich, K., Barbier, A. J., Mullenix, J. B., and Patel, T. B. (1997) *Proc. Natl. Acad. Sci. U.S.A. 94*, 2915−20.
45. Yarfitz, S., and Hurley, J. B. (1994) *J. Biol. Chem. 269*, 14329−32.
46. Lowe, D. G., Dizhoor, A. M., Liu, K., Gu, Q., Spencer, M., Laura, R., Lu, L., and Hurley, J. B. (1995) *Proc. Natl. Acad. Sci. U.S.A. 92*, 5535−9.
47. Dizhoor, A. M., and Hurley, J. B. (1996) *J. Biol. Chem. 271*, 19346−50.
48. Dizhoor, A. M., Boikov, S. G., and Olshevskaya, E. V. (1998) *J. Biol. Chem. 273*, 17311−4.
49. Duda, T., Goraczniak, R., Surgucheva, I., Rudnicka-Nawrot, M., Gorczyca, W. A., Palczewski, K., Sitaramayya, A., Baehr, W., and Sharma, R. K. (1996) *Biochemistry 35*, 8478−82.

BI0110894